

## Adaptation of ANUBIS scheme to SAFARI-1 core characterisation

L. Moloko<sup>1</sup>, C. D'Aletto<sup>2</sup>, J. Di Salvo<sup>2</sup>

1) The South African Nuclear Energy Corporation SOC Ltd (Necsa), P1900, P. O. Box 582  
Pretoria, 0001, SOUTH AFRICA

2) CEA Cadarache – 13108 St-Paul-lez-Durance, FRANCE

Corresponding author: [lesego.moloko@necsa.co.za](mailto:lesego.moloko@necsa.co.za)

**Abstract.** A numerical benchmark project based on the adaptation of ANUBIS scheme to SAFARI-1 research reactor core characterisation has been established under a CEA-Necsa collaboration framework. The objective of the project is to establish a step-by-step numerical benchmarking process through code-to-code comparisons and code-to-experimental data validation. In this paper the preliminary results for the code-to-code numerical benchmark based on APOLLO2 and TRIPOLI4® reference Monte Carlo solution are presented. The results comprise of the standard fuel assembly, control rod assembly and 2D APOLLO2 MOC full core benchmark. The APOLLO2 calculation scheme is based on two level calculation steps, a 172-group self-shielding calculation and 20-group flux calculation based on the XMAS 172-group JEFF3.1.1 cross section library. For this benchmark, the eigenvalues, normalised power distribution and absorption rates were compared. All the calculations are performed at step zero, using fresh fuel assemblies. Although the presence of the in-core irradiation position results in large reactivity discrepancies in a 2D full core calculation, there is good overall agreement between APOLLO2 and TRIPOLI4®.

### 1. Introduction

The South African Nuclear Energy Corporation SOC Ltd (Necsa) and Commissariat à l'Energie Atomique et aux Energies Alternatives (CEA) has established a benchmark project under the CEA-Necsa collaboration framework. The main objective of the project is to adapt the French neutronic calculation scheme, ANUBIS [1], to the SAFARI-1 research reactor core characterisation. The calculation scheme is primarily used to provide calculational support to the OSIRIS experimental reactor, and is based on the use of the APOLLO2 [1], [2] deterministic transport code, and the CRONOS2 code [3], a modular neutronics code which solves the equation of either dynamic or static diffusion or transport of neutrons. Validation and qualification of the scheme have been achieved through comparison to the Monte Carlo TRIPOLI4® reference [4] as well as to the OSIRIS research reactor experimental data [1].

The proposed benchmark project will be achieved through numerical benchmark and qualification using SAFARI-1 experimental data. For the purpose of this benchmark, three phases were identified as follows;

- a. Adaptation of the ANUBIS calculation scheme to the SAFARI-1 research reactor;
- b. Establishment of the code-to-to code numerical benchmark; and
- c. Code to SAFARI-1 experimental data comparison.

The results presented herein are based on phases (a) and (b). At the time of the publication of this paper the results based on a comparison between CRONOS2 and experimental data were not completed. Therefore, the discussion and results herein will be based on APOLLO2 and the reference TRIPOLI4®.

The layout of the paper is as follow; the SAFARI-1 research reactor is briefly described in Section 2, followed by a brief description of the calculational codes in Section 3 and

methodology in Section 4. The results and conclusion are presented in Sections 5 and 6 respectively.

## 2. The SAFARI-1 research reactor

The SAFARI-1 research reactor is a 20 MW tank-in-pool-type material testing (MTR) reactor, the coolant and moderator is light water. The reactor core configuration is shown in *FIG. 1*.

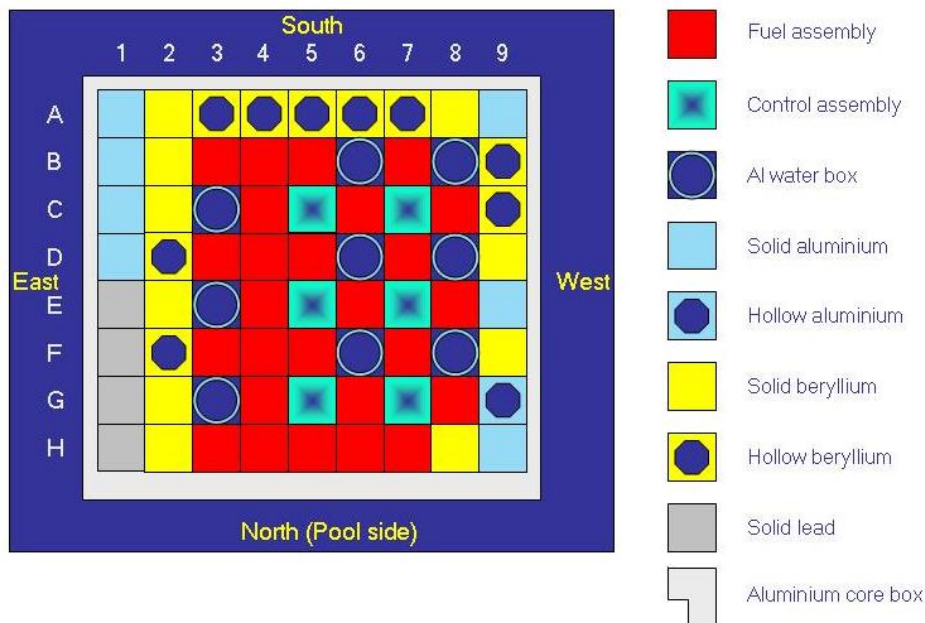


*FIG. 1. SAFARI-1 research reactor core layout*

The reactor has an 8x9 core lattice, housing 26 fuel elements, 6 follower type control rods, a number of solid lead shield elements, solid and hollow aluminium filler elements as well as solid and hollow beryllium reflector elements. The reactor is currently operated with low enriched fuel (LEU), 19.75 % enriched  $U_3Si_2Al$ . The core is fuelled with 19 plate MTR-type fuel elements and the control rods are comprised of a 15 plate fuel follower section beneath a hollow rectangular cadmium absorber section [5].

All the reflector elements, filler elements, water boxes and special devices have the same external dimensions as a fuel element and differ only in internal detail. This provides flexibility for the core layout changes. Each core position has a pitch of 7.71x8.1 cm. The reactor has 9 in-core irradiation positions (shown as the Al water box in *FIG. 1*). The reactor is also equipped with a number of irradiation facilities, such as the hydraulic (i.e., position G9 in *FIG. 1*); non-cadmium and cadmium ringas systems inserted in positions A3 and A4 respectively [5].

Surrounding the core is the aluminium core box, which has the same thickness on the east, south and west side, but somewhat different on the north side (poolside). Some of the routine reactor experiments include control rod calibration, copper-wire activation flux measurements, foils activation flux measurements, etc.

### 3. Calculation codes

A brief description of the APOLLO2 and TRIPOLI4® code systems is presented in Sections 3.1 and 3.2 respectively.

#### 3.1. The APOLLO2 code

The APOLLO2 deterministic neutron transport code is widely used for cross section generation and direct transport calculations, including a wide range of applications in reactor physics. The code uses external multi-group cross section libraries consisting of 99, 172, and 281 groups, respectively. The first corresponds to the energy mesh of the predecessor APOLLO code, the second is the standard XMAS structure [6] and the third is the recently optimised SHEM energy mesh [7]. A typical calculation scheme in APOLLO2 consists mainly of a two-level calculation step, the first is a self-shielding calculation performed in fine energy mesh, followed by the second level calculation, that is, a flux calculation performed on a coarser energy mesh. The choice of the energy mesh is dependent on the external multi-group cross section library used.

APOLLO2 flux solvers are based either on the collision probability ( $P_{ij}$ ) method, the discrete ordinate ( $S_n$ ) method and the method of characteristics (MOC). The MOC in unstructured meshes offers a good accuracy and is known to operate in complicated geometries. All three methods were used in this study. Further details on MOC can be found in references [8], [9], [10].

The first level calculation was performed using the 172-group fine energy mesh cross section library based on the JEFF3.1.1 nuclear data evaluation [11]. The second level calculations were based on the collapsed 20-group coarse energy mesh.

#### 3.2. The TRIPOLI4® reference code

TRIPOLI4® solves the linear Boltzmann equation for neutrons and photons, with the Monte Carlo method. The code uses ENDF format continuous energy cross-sections, from various international evaluations including JEFF-3.1.1, ENDF/B-VII.0, JENDL4 and FENDL2.1. Its official nuclear data library for applications, named CEAV5.1.1, is mainly based on the European evaluation JEFF-3.1.1. The code solves fixed source as well as eigenvalue problems. It is used as a reference tool by CEA as well as its partners.

In this study the TRIPOLI4® reference solutions were obtained using the JEFF3.1.1. A total number of up to  $10^8$  neutron histories were used to reach a good convergence, that is,  $< 10$  pcm in eigenvalues and  $< 10^{-2}$  % in reaction rates.

In order to assure the consistency of the basic nuclear data used in the APOLLO2 and TRIPOLI4® codes, the same evaluation file, JEFF3.1.1, has been chosen.

#### 4. Methodology

A two-step numerical benchmark process has been established in order to validate the APOLLO2 calculation path, starting with an infinite assembly lattice calculation and the second step features a 2D full core calculation. In addition to these steps, validation of the control rod model is considered. Each step of the two-step calculation process is composed of two levels, that is, the first level, which consists of self-shielding calculations and the second level is flux calculations. Detail of the validation process is summarised in the subsequent paragraph.

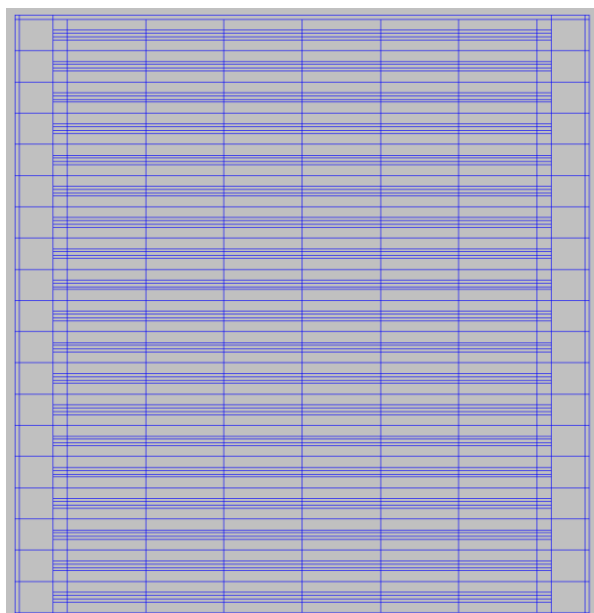
For the two-level standard assembly calculations, the geometry and associated compositions of each component were detailed and the first level self-shielding calculation was performed with a 172-group library on heavy resonant isotopes. In this case a simplified 1D geometry is used. The 172-group flux calculation is then performed on this geometry using the collision probability method. Thereafter, the self-shielded cross sections are collapsed into 20-groups. As a second level step of the calculation, the computed self-shielded cross sections are then redistributed in the exact 2D geometry and the 20-group flux calculation is performed using the exact-2D Pij method. The assembly geometry is composed of 12 meshes (y-direction) in the fuel region and four meshes (x-direction) in each water gap between fuel plates.

For the assembly calculation, the multiplication factor  $k_{\infty}$ , the fission and absorption rates are compared and validated against the TRIPOLI4® results. The comparison of  $k_{\infty}$  is established through the 6-factor formula;

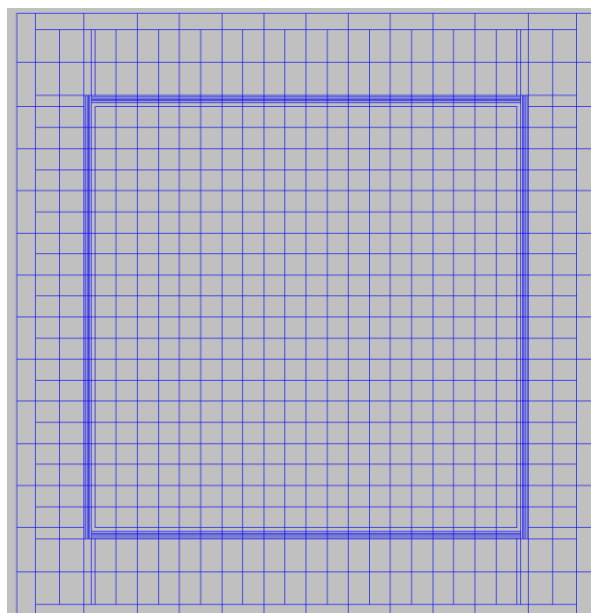
$$k_{\infty} = \chi_{n,2n} \varepsilon_{fast} \varepsilon_{epi} p f \eta$$

where,  $\chi_{n,2n}$  is the total absorption rate (Source  $S = I$ ),  $\varepsilon_{fast}$  is the fast fission factor taking into account even isotopes ( $^{238}\text{U}$ ,  $^{240}\text{Pu}$ ,  $^{242}\text{Pu}$ ) threshold fission, and  $\varepsilon_{epi}$  is the epithermal factor taking into account fission in the resonance range of the odd ( $^{235}\text{U}$ ,  $^{239}\text{Pu}$ ,  $^{241}\text{Pu}$  and  $^{241}\text{Am}$ ). The resonance escape probability is represented by  $p$  and the thermal range below 0.625 eV is characterised by the neutron utilisation factor  $f$  and the neutron reproduction factor  $\eta$ .

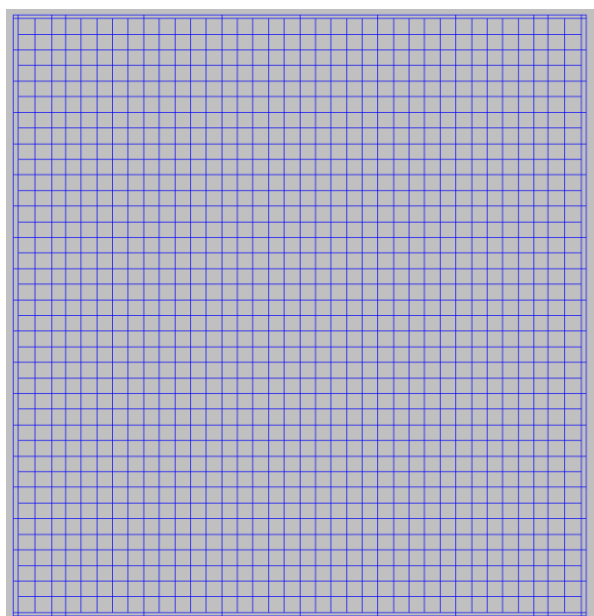
The second step of the numerical benchmark is the MOC calculation, which is based on a 2D SAFARI-1 reactor full core model. In the same way as in the standard assembly calculation, the two-level step was employed, i.e., a 172-group self-shielding calculation performed in 1D simplified geometry followed by a 20-group flux calculation on an exact well segmented geometry generated with SILENE GUI [12]. Examples of the mesh structure used for the standard and control assembly as well as the beryllium reflector element and the ringas system element are shown in *FIG. 2*. The structural element (e.g., solid aluminium, lead element, etc.) use the same mesh as that of the beryllium reflector element.



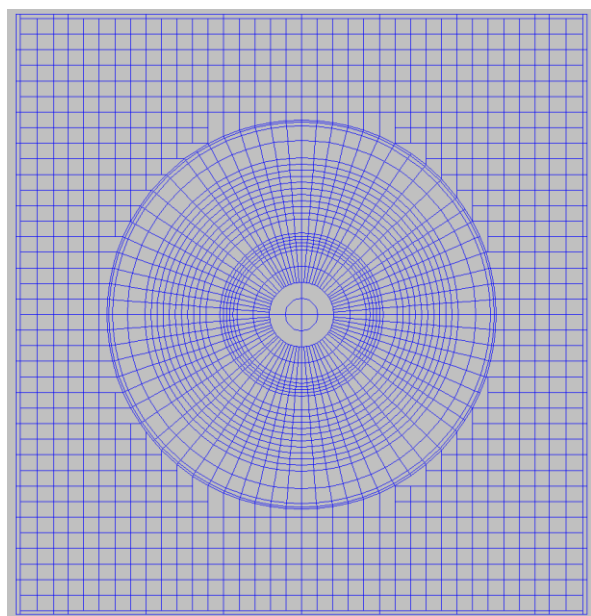
a) Standard fuel assembly



b) Control rod assembly



c) Solid beryllium reflector element



d) Ringas element (A3&amp;A4)

*FIG. 2. Example of the mesh structure for the 2D full core MOC calculation*

The 20 cm pool water modelled around the four sides of the core was divided into meshes of about 0.2 cm for the first 10 cm of the pool from the core box and about 1 cm for the outer 10 cm, except in the north pool side (refer to *FIG. 1.*), where 0.2 cm meshes were used over 20 cm pool water. All the reflectors, experimental and structural assemblies were divided into 20 meshes of about 0.4 cm in both the x and y-direction. Note that this mesh structure was used for the initial studies, it has not been tested to represent an optimum mesh structure – this is reserved for future studies.

In order to validate the full core model and to fully understand the effects associated with various assemblies, four APOLLO2 MOC core configurations were evaluated. The benchmark configuration considered, with reference to *FIG. 1.*, are briefly summarised as follows;

- **Configuration A:** in this case A3 and A4 assemblies are replaced by solid beryllium element. The in-core irradiation positions are replaced by standard fuel assemblies and the control are fully withdrawn – corresponding to follower insertion.
- **Configuration B:** positions A3 and A4 are introduced back into the core, this was done mainly to investigate the effect these assemblies (mainly, the A4 assembly containing a cadmium ring) have on core parameters. The follower assemblies were inserted.
- **Configuration C:** the effect of fully insertion of the 6 control rods was investigated in this case. Configuration B was used with all 6 rods inserted, effectively replacing the follower assemblies.
- **Configuration D:** resembles the introduction of aluminium dummies in the 9-incore irradiation position. Note that the control rods are replaced by the follower assemblies in this case.

The corresponding TRIPOLI4® reference calculations were performed for each of the above-mentioned cases. In this way, the effect on core parameters introduced as a result of each of the above-mentioned configurations, were fully understood.

The MOC parameters used in the full core calculation are shown in Table I. Note that the choice of these parameters was influenced by the accuracy obtained upon comparison with TRIPOLI4® reference.

TABLE I: MOC calculation parameters

MOC parameters option	Core calculation
Azimuthal angles ( $N\phi$ )	24
Tracking step ( $\Delta r$ , cm)	0.04
Bickley polar quadrature, $N\psi$	3
Degree of anisotropy scattering	P0*

Two control rod models were considered as part of these numerical benchmark calculations, that is, the control rod model in an infinite homogenised fuel environment as well as the model in the heterogeneous environment corresponding to Configuration C. For the homogeneous environment model, the APOLLO2 Sn flux calculation was performed with S8 quadrature for the angular approximation and P3 anisotropy scattering (S8P3). The APOLLO2 MOC parameters were as defined in Table I. The normalised absorption rates were compared for the cadmium absorber, the aluminium casing and the water around the control rods.

The results of the numerical benchmark are presented in Section 5. Note that all the comparisons in this study were done at time-step zero. The validation was established by

comparing the multiplication factor ( $k_{\infty}$ ,  $k_{eff}$ ) and the reaction rates to TRIPOLI4® reference solution.

## 5. Results and discussion

### 5.1. Assembly validation results

The results of the 6-factors formula are summarised in Table II.

TABLE II: Comparison of the 2D APOLLO2 with TRIPOLI4®

Six-factors	TRIPOLI4®	(A2-T4)/T4 (pcm)
$\chi_{n,2n}$	1.00029	-8
$\epsilon_{fast}$	1.00651	-9
$\epsilon_{epi}$	1.10744	-75
$p$	0.82162	119
$f$	0.88736	80
$\eta$	2.03012	-6
$k_{\infty}$	1.65029	100

From Table II, it can be seen that there is compensation of errors between  $\epsilon_{epi}$  and  $p$  factors. The overestimation of  $p$  in APOLLO2 can be attributed to the capture rate of  $^{238}\text{U}$  in the resonance range. The error in  $p$  also leads to an increase (overestimation) in the utilisation factor  $f$ . In general, the discrepancies between APOLLO2 and TRIPOLI4® concerning the six factors are satisfactory.

The comparison of reaction rates also showed good agreement. The maximum discrepancy in the fission rate is less than 0.2 % with discrepancies in the absorption rate of about 0.2 % and -0.7 % in the thermal and fast region respectively. Note that the comparison is made relative to TRIPOLI4® and the negative value implies that APOLLO2 is less.

## 5.2. Control rod validation results

The absorption rates of the two control rod models (homogeneous environment – S8P3 and heterogeneous environment – MOC) are summarised in Table III. The results are given for group 1 and 2, the fast and thermal groups respectively.

TABLE III: A2 vs T4 normalised absorption rate for the control rod model

Mediums	(A2-T4)/T4 (%)	
	APOLLO S8P3 (homo. environment)	APOLLO MOC (heter. environment)
Cadmium		
1	1.32	0.19
2	-0.08	-0.01
Water		
1	0.23	6.20
2	-0.02	-0.40
Aluminium		
1	2.42	3.22
2	-1.00	-1.11

The cadmium absorber rod is well accounted for in MOC, however, APOLLO S8P3 has a better overall performance in all three mediums. It can also be seen that the thermal rates are well calculated in both cases. Large discrepancies are observed in the fast energy range, specifically in water and aluminium, with a maximum error of about 6.2 % in MOC calculation.

## 5.3. The 2D MOC results

The results presented herein were obtained by applying reflective boundary conditions on the external boundaries and zero buckling ( $B_2=0$ ). The reactivity effects of the above-mentioned configurations are summarized in Table IV.

TABLE IV: A2 vs T4 computed multiplication factor for 4 configurations

Configurations	TRIPOLI4®	$1/k_{T4} - 1/k_{A2}$ (pcm)
A	1.42078	93
B	1.41626	100
C	1.18192	374
D	1.31023	662

It can be seen from Table IV that Case, A, B and C compares reasonably well with the TRIPOLI4® reference solution. Configuration A is well calculated, with introduction of the ringas system (i.e., positions A3 and A4) resulting in a reactivity effect of about 100 pcm. A consistent decrease in reactivity by about 200 pcm is observed in both TRIPOLI4® and APOLLO2 due to the introduction of the ringas system. This observation is in agreement with previous studies [13].

Insertion of the control rods results in a discrepancy of about 374 pcm, corresponding to the rods efficiency of -14373 pcm and -14100 pcm in TRIPOLI4® and APOLLO2 respectively. This translates to a discrepancy of about 2 % on the total reactivity worth of the control rods.

The dominant effect of 662 pcm is observed in the case of Configuration D – representing the insertion of dummy aluminium in the in-core irradiation position. These discrepancies are mainly due to the large volumes of water in these positions. These results show that the positions are not well accounted for in the APOLLO2 model. As a test case the aluminum dummy models were replaced by blocks of solid aluminium, the discrepancy in the reactivity improved considerably to about 232 pcm. It is clear that the models of these positions in APOLLO2 still need to be improved.

The discrepancies in the reactivity of Table IV can be further understood by comparing the core power distribution. Comparisons of the normalised assembly power distribution are presented in the core maps of FIG. 3. and FIG. 4.

Normalised power TRIPOLI4®  
 Normalised power APOLLO2  
 % Difference (A2-T4)/T4

Configuration A							Configuration B						
	3	4	5	6	7	8		3	4	5	6	7	8
<b>B</b>	0.871	0.975	1.085	1.040	0.946	0.758	0.757	0.833	1.005	1.008	0.936	0.757	
	0.883	0.975	1.075	1.032	0.943	0.769	0.780	0.849	1.001	1.002	0.934	0.770	
	1.4	0.0	-1.0	-0.8	-0.3	1.5	3.0	1.9	-0.4	-0.5	-0.1	1.7	
<b>C</b>	0.996	1.120	1.218	1.199	1.062	0.916	0.947	1.074	1.188	1.187	1.063	0.923	
	1.009	1.119	1.204	1.190	1.058	0.927	0.964	1.078	1.177	1.180	1.060	0.935	
	1.3	-0.1	-1.2	-0.8	-0.4	1.2	1.8	0.4	-1.0	-0.6	-0.3	1.3	
<b>D</b>	1.125	1.228	1.370	1.292	1.179	0.958	1.105	1.216	1.365	1.296	1.193	0.971	
	1.132	1.222	1.346	1.275	1.169	0.966	1.118	1.213	1.344	1.281	1.182	0.980	
	0.7	-0.5	-1.7	-1.3	-0.9	0.9	1.2	-0.2	-1.5	-1.1	-0.9	0.9	
<b>E</b>	1.140	1.254	1.355	1.320	1.147	0.894	1.140	1.260	1.367	1.338	1.167	0.912	
	1.145	1.245	1.329	1.301	1.136	0.903	1.150	1.255	1.345	1.321	1.157	0.922	
	0.4	-0.7	-1.9	-1.4	-1.0	1.0	0.9	-0.4	-1.6	-1.3	-0.9	1.2	
<b>F</b>	1.052	1.127	1.247	1.165	1.047	0.823	1.063	1.143	1.269	1.189	1.071	0.842	
	1.057	1.119	1.224	1.149	1.037	0.833	1.073	1.139	1.249	1.175	1.062	0.854	
	0.5	-0.7	-1.8	-1.4	-1.0	1.2	1.0	-0.3	-1.6	-1.2	-0.8	1.4	
<b>G</b>	0.840	0.914	0.985	0.953	0.830	0.689	0.856	0.934	1.008	0.978	0.852	0.709	
	0.847	0.912	0.970	0.945	0.825	0.700	0.866	0.935	0.996	0.972	0.849	0.721	
	0.8	-0.3	-1.5	-0.8	-0.6	1.6	1.2	0.0	-1.2	-0.6	-0.4	1.6	
<b>H</b>	0.581	0.628	0.687	0.648	0.606		0.594	0.644	0.706	0.667	0.624		
	0.588	0.630	0.684	0.647	0.610		0.604	0.648	0.704	0.667	0.629		
	1.3	0.3	-0.5	-0.1	0.5		1.7	0.7	-0.2	0.1	0.8		

FIG. 3. Deviation of the normalised assembly power distribution from the TRIPOLI4® reference

FIG.3. shows normalized core power distribution for configuration A and B. Note that the difference between these configurations is the solid beryllium elements (positions A3 and A4) in configuration A which are replaced with detailed models of the ringas system in configuration B.

It can be seen that the power peaking is consistent in both TRIPOLI4® and APOLLO2, that is, towards the centre around the assemblies D5 and E5. The maximum difference of up to 3 % is observed in assembly B3 (Configuration B) due to the introduction of the ringas system. These assemblies are seen to have important local effects on the neighbouring fuel assemblies,

that is, an increased discrepancy in power distribution of 3.0 % and 1.9 % (see Configuration B) in fuel assembly neighbours B3 and B4 respectively. The global impact of the ringas system seems to be somewhat less important. Generally, the standard and follower assemblies are well accounted for and the normalised assembly power distribution comparisons are satisfactory.

Perturbations due to the introduction of the control rods and in-core irradiation position are shown in the maps of FIG. 4.

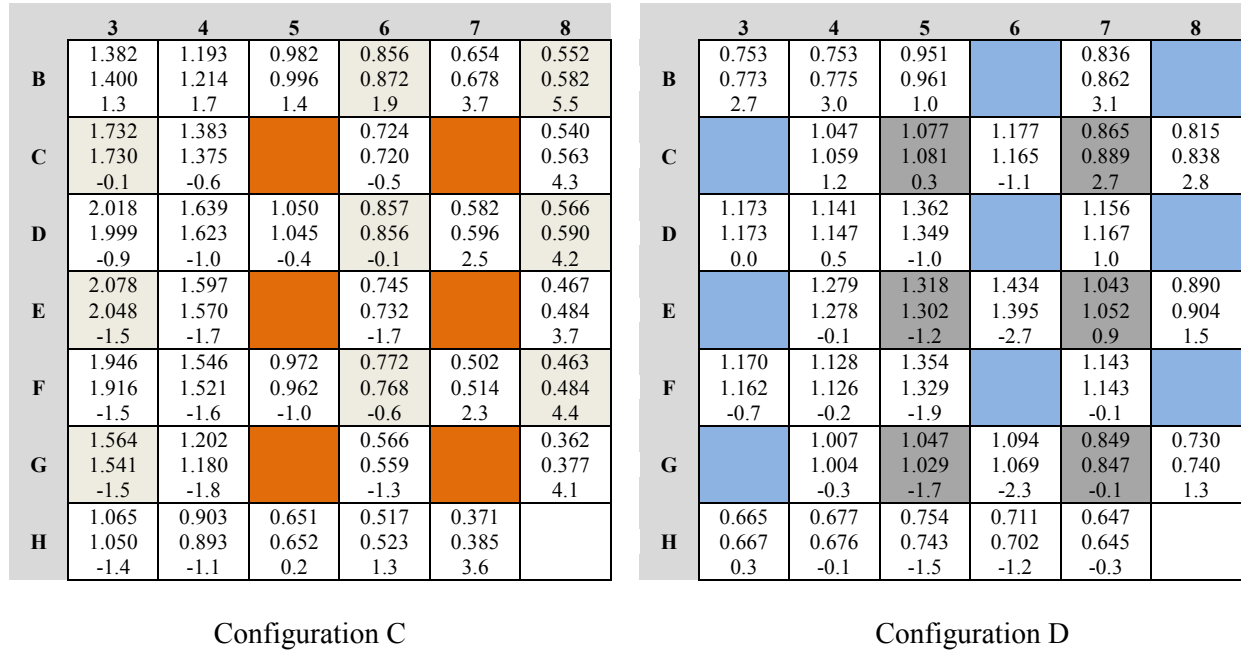


FIG. 4. Deviation of the normalised assembly power distribution from the TRIPOLI4® reference

Configuration C, which comprises of the introduction of 6 control rods, results in a power tilt towards the periphery of the core, mainly in columns 3 and 4 of FIG. 4. The maximum errors are observed along column 8 with the assembly power peak shifted to assembly position E3 in both TRIPOLI4® and APOLLO2. The discrepancies observed in this case can also be attributed to the errors in the MOC absorption rates observed in Table III.

On the other hand, the irradiation positions in Configuration D, do not lead to any pronounced effects in both the local and global assembly power distribution.

Generally, it can be seen that the power distribution calculated by the two codes agree well to within 2 % and 3 % for Configuration A and B respectively. Configuration C result in a large differences of up to 5.5 %, with differences within 3 % observed in Configuration D. Despite the large errors observed in Configuration C, both TRIPOLI4® and APOLLO2 models are consistent. The comparison of all four cases appears to be promising and consistent with the reference solution TRIPOLI4®.

The calculation times for the 2D full core MOC calculations (Configurations A, B, C and D) are shown in Table V. The calculations were performed on a AMD Opteron Linux DELL

2.8Ghz computer. The TRIPOLI4® calculations were performed in parallel mode using 64 processors.

TABLE V: CPU time in APOLLO2 and TRIPOLI4®

Solvers	20g MOC	TRIPOLI4®
	CPU times (s)	
A	3885	18198
B	3290	17495
C	5837	14524
D	2223	15593

## 6. Summary and Conclusions

The two phases of the benchmark project have been presented, that is, adaptation of the ANUBIS scheme to the SAFARI-1 research reactor and numerical benchmark based on APOLLO2 and the reference TRIPOLI4® solutions. These two phases form an integral part of the benchmark calculation, thus a considerable amount of time has been spend towards completing them. Although the phases are partially completed, through a step-wise process employed in this benchmark, important observations were made and sources of error identified for future improvement.

The assembly calculation results showed an acceptable TRIPOLI4® -APOLLO2 agreement in  $k_{\infty}$ , as well as in reaction rates. Furthermore, the standard and follower assembly results in the APOLLO2 MOC calculation are predicted accurately. The control rod models are satisfactory, however, further improvement could be considered.

On the other hand, the most important source of error upon comparisons with TRIPOLI4® has been identified to be in the control rods and the irradiation positions models. The large discrepancies observed in these cases warrant without a doubt, careful consideration for future improvement.

In general, the APOLLO2 code is shown to produce very promising results when adapted to the 2D SAFARI-1 reactor models. Future improvements include, but are not limited to, improved models of the in-core irradiation positions and control rod assemblies. The optimisation of both geometry mesh as well as the energy mesh (i.e., 281 groups SLEM energy mesh) is also envisaged for future studies. Completion of phases (b) and (c) is planned for the near future.

## 7. References

- [1] Gueton, O., et al., Validation and qualification of the ANUBIS scheme used for safety assessment and operation management of the OSIRIS reactor, IGORR12 Conference, Beijing (China), October 28 – 30, 2009.
- [2] Sanchez, R., et al., APOLLO2 year 2010, Nuclear Engineering and Technology, Vol. 42, NO. 5, October 2010, 474 – 499.
- [3] Lautard, J. J., et al., “CRONOS: a modular computational system for neutronic core calculations”, *IAEA Specialists Meeting on Advanced Computational Methods for Power Reactors*, Cadarache, France September, 1990.
- [4] Brun, E., et al., “Overview of TRIPOLI4® version 7 continuous-energy Monte Carlo transport code,” Proc. Int. Conf. ICAPP 2011, Nice, France (2011).
- [5] D’Arcy, A. J., Description of the SAFARI-1 Reactor, Safety Analysis Report, Chapter 5, RR-SAR-0005, Necsa, August 2000.
- [6] Dean, C. J., et al., “Weighting spectra for Xmas group scheme”, Winfrith Technology Center, 1990.
- [7] Hfaiedh, N., Santamarina, A., “Determination of the optimised SHEM mesh for transport calculation,” Proc. Int. Top. Mtg. on Mathematics and Computation, Supercomputing, Reactor Physics and Nuclear and Biological Applications (M&C2005), Avignon, France, September 12 – 15, 2005.
- [8] Févotte, F., et al., “Improved transmission probabilities for the neutron transport problem with method of characteristics in APOLLO,” 2<sup>nd</sup> International Youth Conference on Energetics (IYCE 2007), Budapest, Hungary, 31 May – 2 June, 2007.
- [9] Aggery, A., “The characteristics method applied to a MTR whole core modelling”, PHYSOR2004, Chicago, Illinois, April 25 – 29, 2004.
- [10] Di Salvo, J. et al., The Osiris reactor neutronic reference calculation scheme based on the method of characteristics, PHYTRA1: First International Conference on Physics and Technology of Reactors and Applications, Marrakech, Morocco, March 14 – 16, 2007, GMTR (2007).
- [11] Santamarina, A., et al., “The JEFF-3.1.1 nuclear data library”, NEA, JEFF Report 22, 2009.
- [12] Stankovski, Z., “La java de Silene: A Graphical User Interface for 3D Pre & Post Processing”, joint International Conference on Mathematical Methods and Supercomputing for Nuclear Applications, Saratoga Springs, NY USA, October 6 – 10, 1997.
- [13] Moloko L.E. et al., Improved SAFARI-1 research reactor irradiation position modeling in OSCAR-3 code system, IEEE Transactions of Nuclear Science, Vol. 58, NO. 4, August 2011, 1907 – 1912.